CrystEngComm

Accepted Manuscript

ROYAL SOCIETY OF CHEMISTRY

www.rsc.org/crystengcomm

Complex three-dimensional lanthanide metal-organic frameworks with variable coordination spheres based on pyrazine-2,3,5,6-tetracarboxylate

Conrad W. Ingram[1*], Geoffrey Kibakaya[1], John Bacsa[2], Stephan R. Mathis,II[1], Alvin A. Holder[3], Varma H. Rambaran[4], Brandon Dennis[1], Esmeralda Castaneda[1], Julianne S. Robbins[5] and Z. John Zhang[5]

[1] *Center for Functional Nanoscale Materials, Department of Chemistry, Clark Atlanta University, Atlanta, GA 30314, U.S.A.*

[2] *Department of Chemistry, Emory University, Atlanta, GA 30322, U.S.A.*

[3] *Department of Chemistry and Biochemistry, Old Dominion University, Norfolk, VA 23529, U.S.A.*

[4] *Biomedical Engineering Unit, The University of Trinidad and Tobago, Lots 74-98, O'Meara Industrial Park, Arima, Trinidad, West Indies*

[5] *School of Chemistry and Biochemistry, Georgia Institute of Technology, Atlanta, GA 30332, U.S.A.*

Corresponding author: Tel.: +1 404-880-6898; E-mail address:*cingram@cau.edu

Abstract

Metal-organic frameworks $\{[Ln_4(pztc)_3(H_2O)_{11}]\bullet 10(H_2O)\}_n$ (Ln = Gd(**1**), Tb(**2**); pztc = pyrazine-2,3,5,6-tetracarboxylate) containing variable coordination spheres and with a complex and unusual three dimensional structure, were synthesized by the reaction of H_4pztc with the respective Ln(III) salt in water under hydrothermal conditions. The compounds were characterized by single crystal X-ray crystallography, elemental and thermal analysis, and FTIR spectroscopy. The asymmetric units in these compounds have four symmetry-independent Ln(III) ions and these are octa- and nona-coordinate centers, with irregular coordination polyhedra from $[Ln(pztc)_2(H_2O)_6]$, $[Ln(pztc)_2(H_2O)_4]$, $[Ln(pztc)_3(H_2O)_3]$, $[Ln(pztc)_3(H_2O)]$, and $[Ln(pztc)_4]$ cluster units. The fully deprotonated ligand, pztc, coordinates to the Ln^{3+} ions through seven or through ten of its atoms (*i.e.,* the maximum coordination number for this ligand). The three-dimensional open framework contains irregular channels along the [001] crystallographic direction. The channels are approximately 12 Å wide at their largest dimension and contain strongly hydrogen bonded water molecules of crystallization which further stabilize the structure. The solvent accessible volume is 20 % of the total volume. The structures exhibit magnetic behavior that is characteristic of the respective isolated paramagnetic lanthanide ions.

Introduction

The design and preparation of coordination polymers (CPs) and metal organic frameworks (MOFs), particularly those containing open channels and pores, are of great interest for applications in heterogeneous catalysis, gas adsorption, storage, and separation, magnetism, and optical sensing.[1-4] We are interested in assembling high dimensional open MOFs structures from lanthanide ions and small multi-topic ligands. The optical and magnetic properties arising from f-f transitions in the lanthanide elements have sparked great interest in the synthesis of lanthanide-MOF structures.[4e-g] The lanthanide ions, however, can pose significant challenges in directing the structure of the products, due to their propensity for high and variable coordination numbers.

In targeting organic linkers for the construction of open framework MOFs, the multi-topic aromatic polycarboxylic acid, pyrazine-2,3,5,6- tetracarboxylic acid (H_4pztc) is very intriguing because of its rigidity, high symmetry, and the presence of ten (N and/or O) donor atoms. This ligand is among the linkers of highest denticities used in CPs and MOFs synthesis, and therefore possesses the characteristics to produce polymeric networks with wide structural diversity. The fully deprotonated ligand is widely reported for the synthesis of CPs and MOFs mainly in combination with selected s- and d- block metal ions. Among the s-block metals are Li,[5, 6] Na, K, Cs,[7] Ca[8], and Mg[9], whereas the d block metals include Co[10] and Cu,[11-15] alkali metal-Cu,[16] Mn,[17-19] Fe,[20] Ni,[21,22] Ti,[23] Cd,[24-26] and Ag[27]. All, except Cd, crystallize as 1-D chains or 2-D layered CPs. In some cases the structures extend into 3-D networks through hydrogen bonding. A covalently bonded 3-D dense non-porous network was reported for Cd.[24]

Zhang *et al*. reported the synthesis of heterometallic isostructural pztc-MOFs, namely, Ln-K (Ln = Ho, Dy, and Yb),[28] and Ln-Na (Ln = Ce, Sm, Eu, Gd, and Tb) [29] with both series possessing 3-D arrangements with 1-D channels. Thuery and Masci also reported a heterometallic 3-D structure containing Eu-K-pztc, which is devoid of channels and pores. [30] They also reported the use of the actinide element, uranium, (as UO_2 species) in the synthesis of a 3-D $(UO_2)_2$- pztc MOF structure.[31] Yang *et al*. synthesized a 2-D layered Tb-pztc that retained its structural integrity when the inter layer water molecules are removed[32]. To date, there is only one report of 3-D open framework structures that contains a homo-metallic lanthanide ion and the pztc ligand. Quan *et al*. reported the synthesis of isostructural 3-D Ln-pztc (Ln = Yb, Lu, and Er) MOFs containing water clusters within their 1-D channels.[33]

In several of the reported pztc-containing structures, it is observed that water molecules added as a solvent to the synthesis mixtures also serve as a co-ligand and coordinates the metal ions within the structures. Further, several of the reported structures, contain pztc in combination with other co-ligands, including, pyridine[11,22,25] and 2,2'-bpyridine[27]. It also noteworthy that partial deprotonation of H_4pztc to H_2pztc^{2-} can occur during synthesis, leading to significant intra-ligand hydrogen bonding within the resulting MOF and CP structures.[19,20] This may limit the extent of multidimensional connectivity that could otherwise be attained.

We herein report the synthesis of two new isostructural 3-D open framework lanthanide MOFs, $\{[Ln_4(pztc)_3(H_2O)_{11}]\bullet 10(H_2O)\}_n$ (Ln = Gd(**1**) and Tb(**2**)), that contain pztc and a homometallic lanthanide ion. The ligand exhibits four different coordination modes, its highest observed in CPs and MOFs. This, in combination with four crystallographically independent lanthanide ions present, results in a highly complex connectivity that generates a unique variety of cluster units, namely, $Ln(pztc)_2(H_2O)_6]$, $[Ln(pztc)_2(H_2O)_4]$, $[Ln(pztc)_3(H_2O)_3]$, $[Ln(pztc)_3(H_2O)]$, and $[Ln(pztc)_4]$ within the structures. The structures contains channels that are approximately 12 Å wide at their largest dimension, and within which strongly hydrogen bonded water molecules of crystallization that further stabilize the framework are present. The structures exhibit magnetic behavior that is characteristic of the respective isolated non-interacting paramagnetic lanthanide ions.

Experimental section

Synthesis

General method and materials: Pyrazine-2,3,5,6-tetracarboxylic acid was synthesized according to published procedure.[34] The other chemicals were purchased from commercial suppliers and used without further purification.

*Synthesis of **1** and **2**.* Structures **1** and **2** were synthesized in a similar manner under hydrothermal conditions. In the synthesis of **1**, 12.8 mL of a 3.9 mM aqueous solution of H_4pztc (12.8 mg, 0.050 mmol), and $Gd(NO_3)_3\bullet 6H_2O$ (16.9 mg, 0.036 mmol) were sealed in a 20 mL glass vial and heated in an oven at 85 °C for 4 days. The needle-like crystalline product was collected by filtration and washed with deionized H_2O. The ligand to metal mole ratio in the synthesis mixture was 1:0.75 for both **1** and **2**. The synthesis yield, chemical composition, and Fourier - transformed infrared (FTIR) spectral features are as follows:

$\{[Gd_4(C_8N_2O_8)_3(H_2O)_{11}]\cdot 10H_2O\}_n$ (**1**). Yield = 45 %. Elemental anal. Found: C, 16.48; H, 2.26; N, 3.71 %. Calc.: C, 16.35; H, 2.40; N, 4.77. FTIR (cm^{-1}): 3420 (s,br), 3200 (s, br), 1622 (s), 1400 (s), 1328 (m), 1155 (m), 876 (w), 828 (w), 592 (w).

$\{[Tb_4(C_8N_2O_8)_3(H_2O)_{11}]\cdot 10H_2O\}_n$ (**2**). Yield = 60%. Elemental anal. Found: C, 16.38; H, 2.13; N, 4.84. Calc.: C, 16.28; H, 2.39; N, 4.75 %; FTIR (cm^{-1}): 3420(s,br), 3200(s, br), 1629(s), 1406(s), 1328(m), 1195(w), 1159(m), 881(m), 829(m), 773(w), 633(w), 595(w), 498(w).

Characterization techniques

Suitable crystals of **1** and **2** were selected and mounted on a Bruker APEX-II CCD diffractometer equipped with an Oxford Cryosystems low-temperature cryostream operating at T = 110(2) K. The structures were solved with Superflip using the charge flipping algorithm[35] and by using Olex2[36] as the graphical interface. The crystals of **1** (and **2**) are twinned non-merohedrally. The diffraction for **2** was much weaker than **1** with multiple rotational twining. The model was refined with the Shelxl[37] refinement program. The atomic coordinates for **1** were used for the refinements of **2** with Gd replaced by Tb. The results for the refinements are shown in Table 1. Although the twin law for **1** was a perfect 180 degree rotation about the (010) reciprocal direction, about half of the reflections were composite reflections and were difficult to integrate and scale. The large residual peaks are due to the twinning. The faces could not be measured and a numerical (face-indexed) absorption correction could not be applied due to the twinning. As the material absorbs strongly, small errors due to twinning had a large effect on the residual densities. Hydrogen atoms were placed in geometrically idealized positions and in suitable locations for forming hydrogen bonds to donor oxygen atoms. The compound contains 10 water molecules that are not directly bonded to the metal ions, but are strongly hydrogen bonded to each other. Some of these waters are disordered and the distances between hydrogen atoms are short. In the case of **2,** a total of 874 restraints (mainly atomic displacement RIGU and ISOR restraints) were used to refine the structure.

Powdered X-ray diffraction (PXRD) was conducted on a Panalytical Empyrean Series 2 Diffractometer, using Cu Kα radiation, Bragg-Brentano optics, a Pixel 3-D area detector, and with voltage and current settings of 45 kV and 40 mA, respectively. FTIR measurements were recorded on the neat samples on a Bruker Alpha-P FTIR spectrophotometer (intensive pattern: m-medium, s-strong, and w-weak). Thermogravimetric analysis (TGA) was conducted on a TA Instrument Q50 thermal analyzer. The solids were heated at a rate of 5 ºC/min from ambient temperature to 700 ºC under air flow. Temperature dependent magnetization measurements were carried out on a superconducting quantum interference device (SQUID) magnetometer (Quantum Design MPMS-5S) in the range of 5K-320 K under an applied field strength of 1000 Oe. The samples were prepared by fully dispersing an appropriate amount of dry powder in eicosane. Elemental analysis was performed at Atlantic Microlab, Atlanta, GA, USA.

Results and discussion

Synthesis

The colorless products obtained were of small needle-like morphology. In addition to the ligand to metal mole ratio of 1:0.75 used for the structures of **1** and **2**, syntheses were also conducted using ratios of 1:1.3, 1:1.5 and 1:2.0. Powdered XRD and single crystal X-Ray crystallography revealed that all products from these ratios are isostructural with **1** and **2**. It is noteworthy that full deprotonation of the ligand occurs in the synthesis of these structures, without the addition of a base to synthesis mixtures. This is in contrast to reported synthesis of other 3-D pztc structures during which a base is usually added.[24,28-33] Also, in our attempts to synthesize structures that incorporate 3,6-dimethylpyrazine-2,5-dicarboxylate and/or 2,2’- bpyridine as co-ligands in similar mole ratios as above, it was observed that the structures were resistant to incorporating these additional ligands under the synthesis conditions explored, as indicated by single crystal X-Ray analysis.

Crystal structure description

Compounds **1** and **2** are isostructural. The diffraction for **1** was significantly better than **2,** hence the structure of **1** will be discussed in detail. Selected bond lengths and bond angles for **1** are shown in Table 2. The lists of bond lengths, bond angles and other structural details are provided as electronic supplemental information (ESI). The structure is a complex 3-D metal organic framework consisting of four topologically inequivalent Gd(III) ions, four pyrazine tetracarboxylate ligands, eleven coordinated water and ten lattice water molecules (Fig. 1).

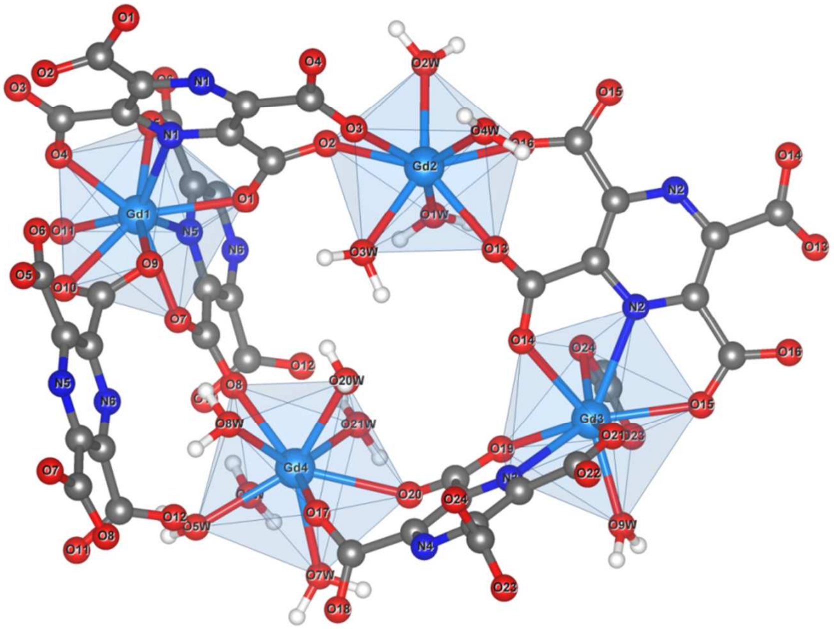

Fig.1. A diagram showing the four different gadolinium ions, the four inequivalent pyrazine molecules, and the bound water molecules in the crystal structure of **1**.

The gadolinium ions have variable coordination numbers and irregular coordination polyhedra based on the calculated bond angle variance and mean quadratic elongation.[38] The Gd-O bond distances vary within the range of 2.333(4) to 2.662(3) Å (Table 2). The bond length and angle variations are accommodated because the electronic effects are small and the atomic 4f shell does not contribute much to the chemical bonding. The interaction between the metal ion and the ligands is primarily electrostatic. Thus, in these cases steric and packing effects override electronic effects, or at least play a prominent role in determining bond angles. The large size of the lanthanide ion and the ligand's high denticity facilitate variable geometries and high coordination numbers (eight and nine). The presence of coordinated water molecules is also a contributing factor.

Metal coordination: The coordination number of the gadolinium, Gd1, is nine with seven oxygen and two nitrogen atoms from four surrounding pyrazine ligands, and the GdN_2O_7 polyhedron is an irregular tricapped trigonal prism (Fig. 2a).[39] It is the only gadolinium ion in the structure without oxygens from water molecules. Four pyrazine ligands donate seven oxygen atoms as follows: one pyrazine contributes a carboxylate group in k^2-O_2 chelating mode, a second contributes one oxygen atom from a carboxylate group in k-O mode, and the third (and fourth) ligand contributes one oxygen each from two of its carboxylates that are *ortho* to a ring-nitrogen. For the third and fourth ligand, the two *ortho* oxygen atoms and the nitrogen atom, bind the metal in tridentate k^3-O'NO"-

chelating mode. This -ONO- coordination mode is also observed in 3-D uranyl and cadmium coordination polymers.[24,31] The Gd-O bond lengths range from 2.344 (3) to 2.506(3) Å and the Gd1-N bond lengths range from 2.519(3) to 2.611(3) Å [average bond length is 2.45 (3) Å], while the O-Gd-O angles range from 54.4 (1) to 84.9(1)° (Table 2).

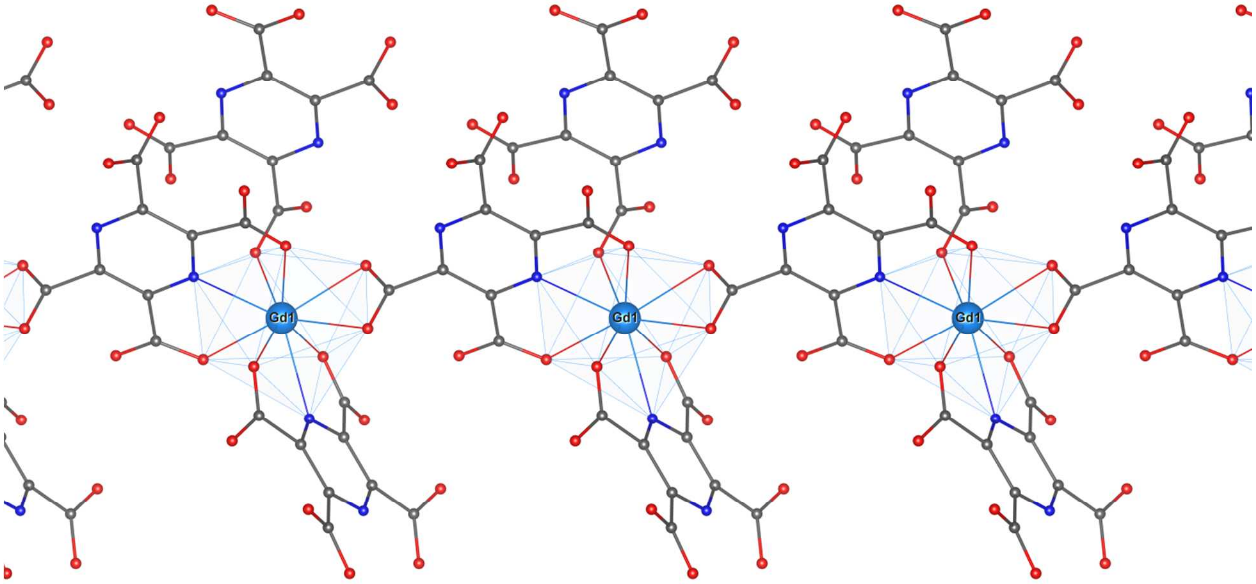

Fig. 2a.

The second symmetry independent metal, Gd(2), coordinates eight oxygen atoms with the GdO_8 polyhedron in a more regular square antiprism geometry. Four of these oxygens are from monodentate water molecules (Fig. 2b). The remaining four oxygens are from two pyrazine tetracarboxylate ligands, with each ligand contributing one O atom in *k*-O mode from each of two adjacent carboxylate groups. The Gd-O bond lengths range between 2.333(3) Å and 2.421(3) Å.

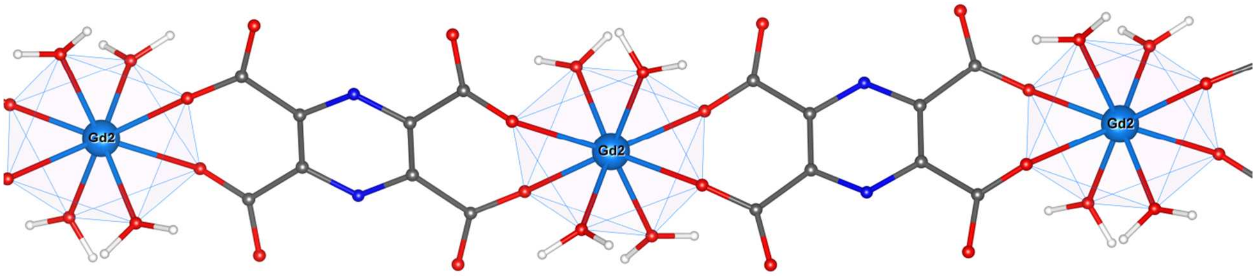

Fig. 2b.

Gd(3) is nine coordinate with seven oxygen atoms and two nitrogen atoms in an irregular tricapped trigonal prism geometry (Fig. 2c). Four oxygens and two nitrogens are from two pztc ligands, with each ligand in tridentate k^3-O'NO" chelating mode involving single oxygen atoms from two of its carboxylates, and the adjacent nitrogen atom of the pyrazine ring. Two Gd-O bonds are from the carboxylate oxygens of a third bridging ligand in bidentate k^2- *O'O"* chelating mode. The Gd3-O bond lengths range between 2.376(3) Å and 2.490(3) and the Gd3-N bond lengths range from 2.520(3) to 2.662(3) Å. The ninth bond is with an oxygen from one coordinated water molecule, with Gd3-O(9W) bond length of 2.400(3) Å.

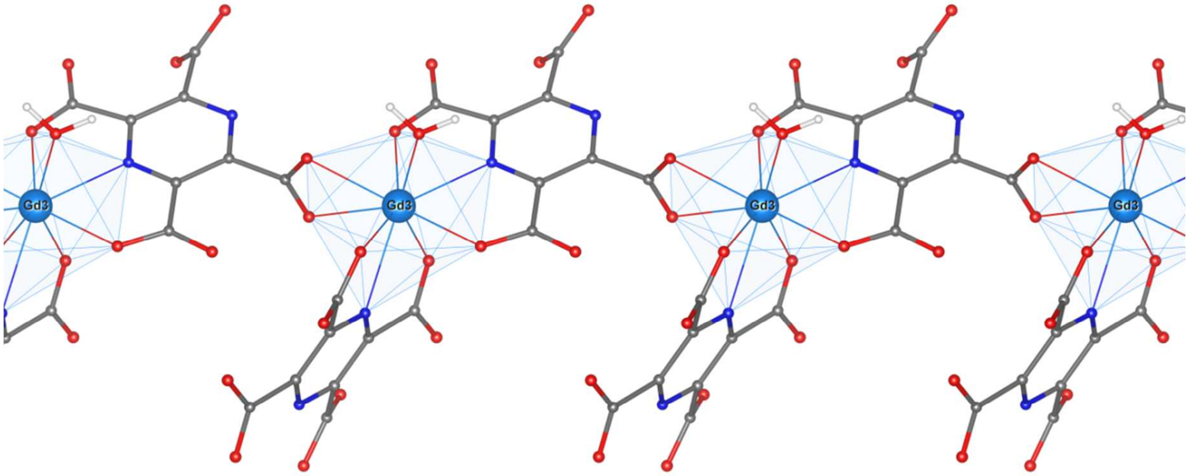

Fig. 2c.

The fourth symmetry independent metal, Gd4 is nine coordinate with a distorted tricapped trigonal prism geometry (Fig. 2d). This ion is highly hydrated: Six Gd-O bonds are with the oxygen atoms of six coordinated water molecules with Gd4-O(W) bond lengths ranging between 2.393(3) to 2.507(3) Å. Presumably, this range in distances is dictated by hydrogen bonding and ligand-ligand repulsions. Two bonds to oxygens are formed with one pztc ligand. The ligand contributes one oxygen atom from each of two adjacent carboxylate groups. The third Gd-O bond is with a carboxylate oxygen of a second pztc ligand. The Gd4-O bond lengths range between 2.339(3) and 2.541(3) Å.

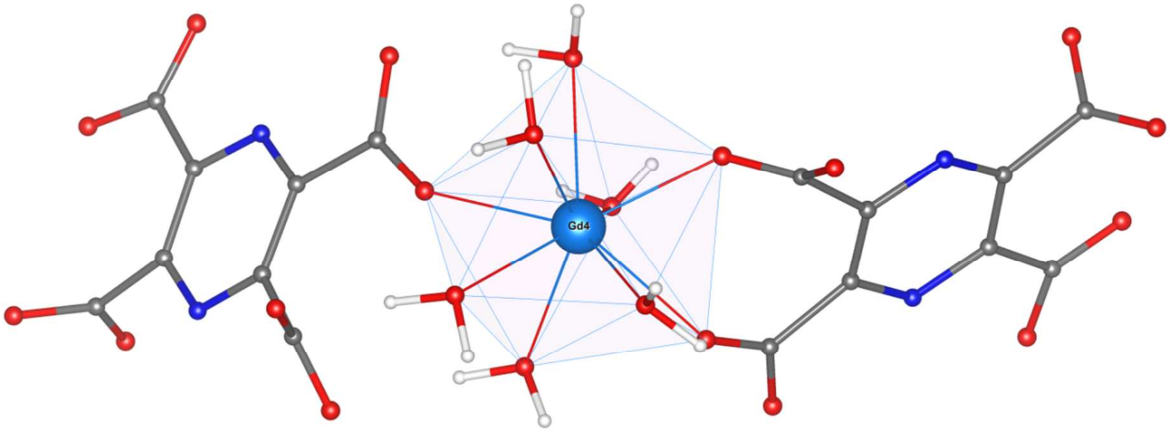

Fig. 2d.

Fig. 2. Coordination environments of the 4-different gadolinium ions, (a) Gd1, (b) Gd2, (c) Gd3, and (d) Gd4.

The observed Gd-O bond lengths are within the range typically reported for Gd-MOFs with oxygen-containing ligands.[40-43] Likewise, the Gd-N bond lengths are within the range typically reported for Gd- MOFs with nitrogen-containing ligands.[44,45] Compound **2** shows bond angles and bond lengths (Tables S1-S3) similar to those that are generally reported for Tb-N, Tb-O or Tb-ONO coordination in MOFs.[46] This wide range in bond distances associated with the multiple coordination modes of the ligands is significant and results in the complex network structure.

Ligand coordination: There are four inequivalent pztc ligands (and eleven inequivalent water molecules) and four different complexing gadolinium atoms. Two pyrazine tetracarboxylate ligands coordinate as decadentate and the other two are heptadentate (Fig. 3). Both decadentate pyrazine tetracarboxylates are μ_4-ligands (each coordinates 4 metal atoms, with 2 metal atoms by two donor atoms and 2 metal atoms by three donor atoms).

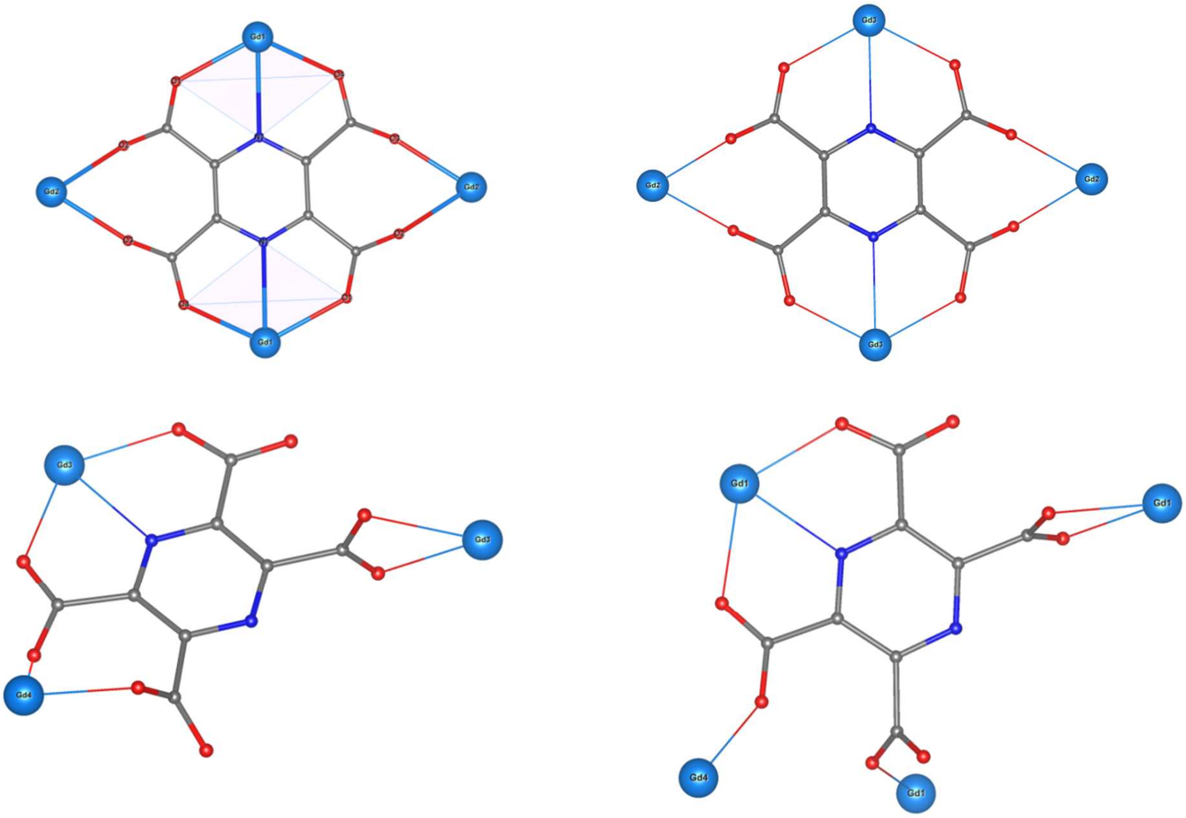

Fig. 3. Coordination modes of pztc.

One heptadentate pyrazine is a µ3-ligand, coordinating two metal atoms by two donor atoms, and one metal atom by three donor atoms of the ligand. The second heptadentate pyrazine is a µ4-ligand. It coordinates two metal atoms with one donor atom, one metal atom by two donor atoms, and one metal atom by three donor atoms. This diverse combination of coordination modes by pztc, represents a first for this ligand in MOFs, to the best of our knowledge.

Two subnets are visible when the structure is projected on the (100) plane, and these are linked by the hydrated gadolinium ions, Gd2 and by Gd4 (Fig. 4).

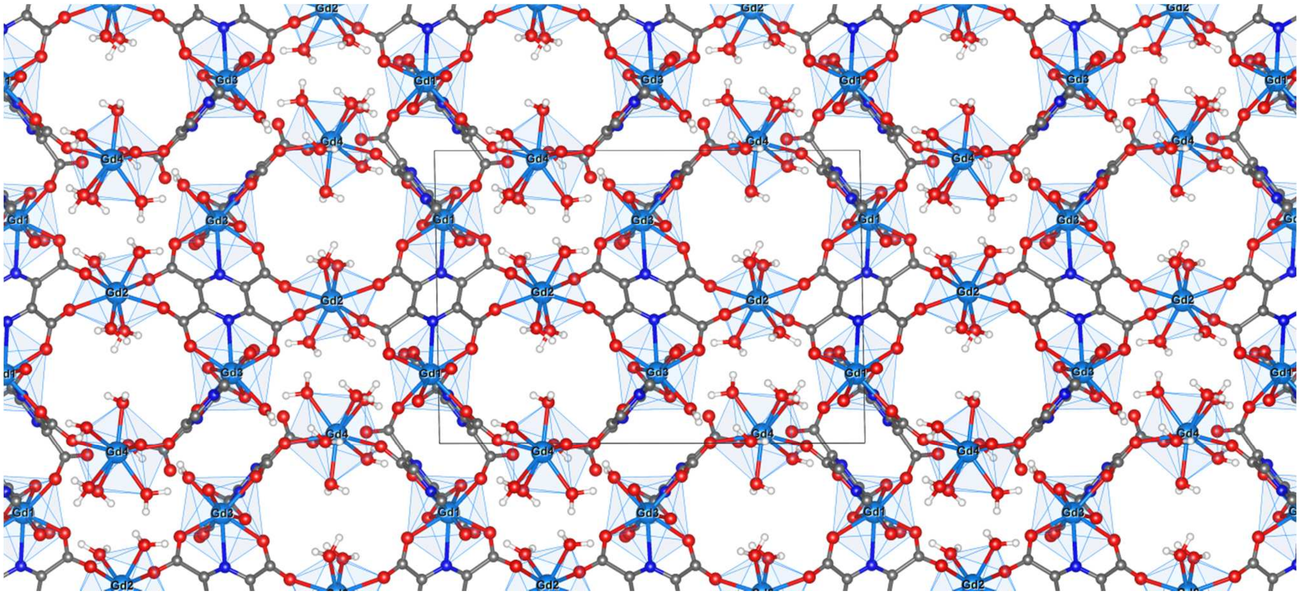

Fig.4. The structure of $\{(Gd_4(pztc)_3(H_2O)_{11}\bullet 10(H_2O)\}_n$ viewed along the *a*-axis.

The first subnet is an infinite two-dimensional layer of nine coordinate gadolinium ions (Gd1) bridged by pyrazine ligands parallel to the (001) plane (Fig. 5).

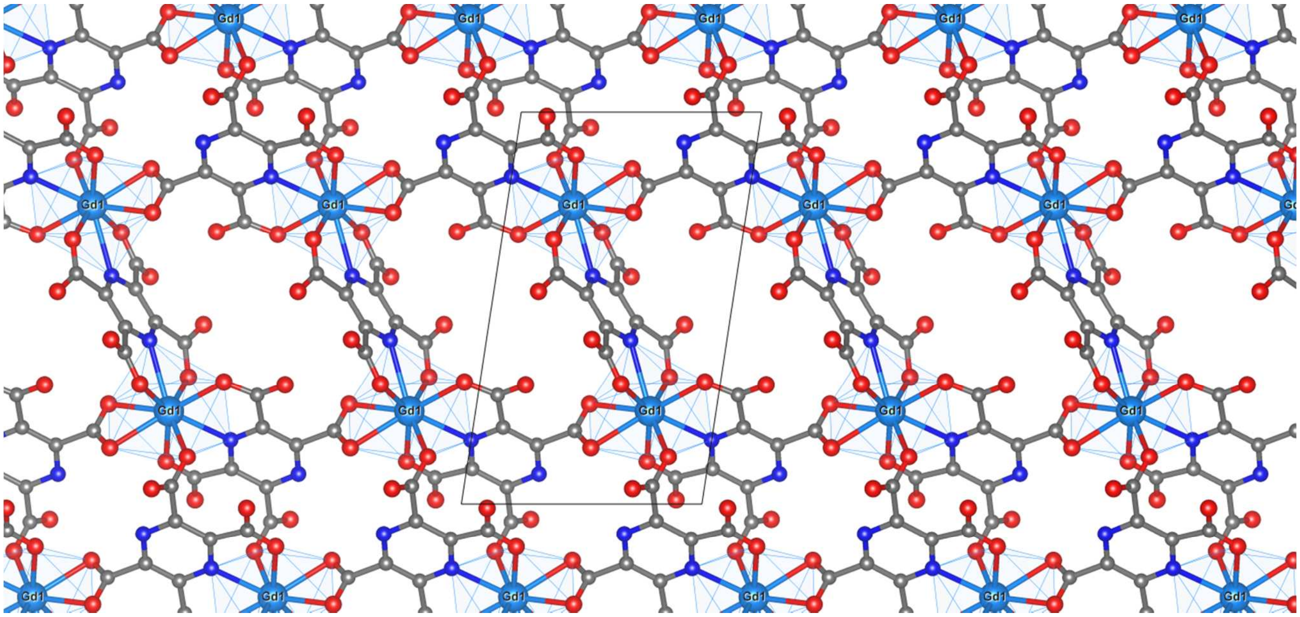

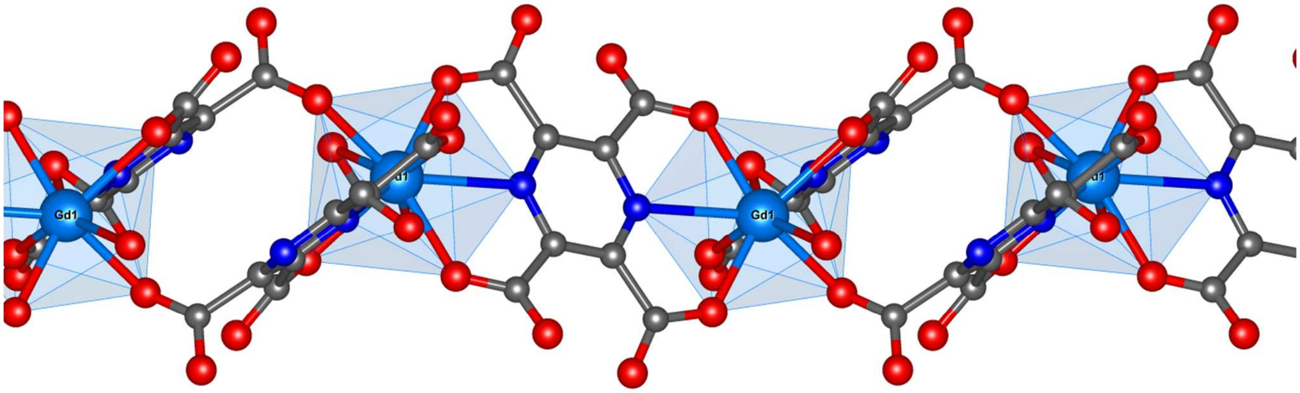

Fig.5. A subnet consisting of an infinite two-dimensional layer of nine coordinate gadolinium ions (Gd1) bridged by pyrazine tetracarboxylate ligands viewed along the *a*-axis (top) and the *c*-axis (bottom).

The second subnet is an infinite one-dimensional chain consisting of gadolinium ions (Gd3) bridged by pyrazine ligands (along [100]). The polymeric chain consists of two chains cross linked by pyrazine ligands. The chains form strong hydrogen bonds to each other to form an infinite two-dimensional layer in the *ab*-plane (Fig. 6a).

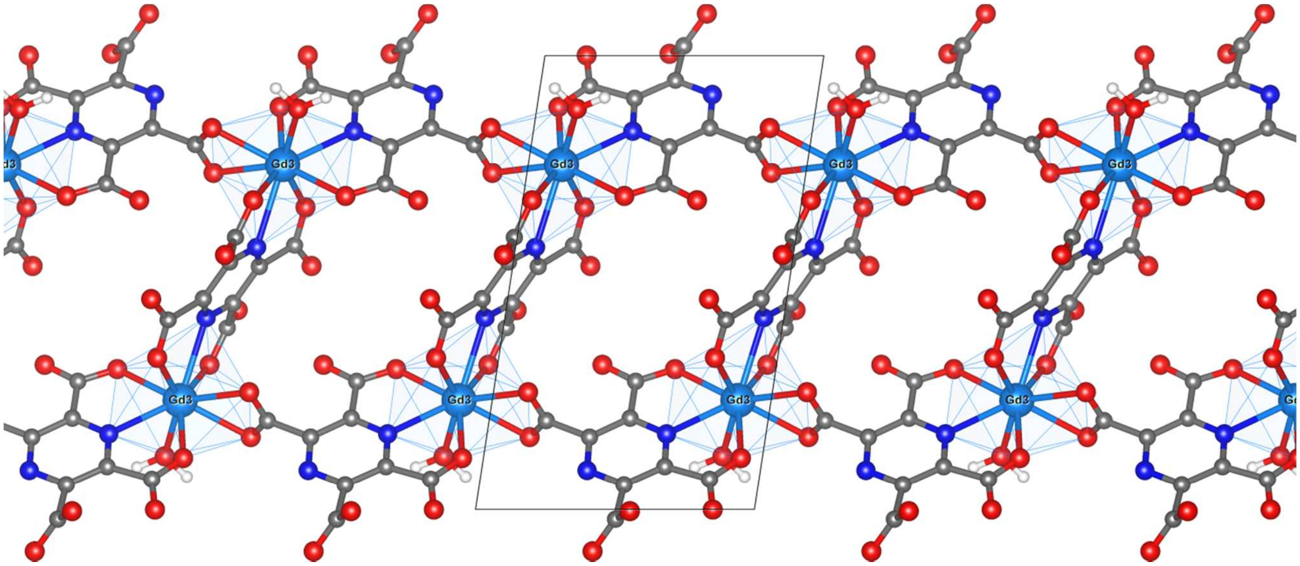

Fig. 6a.

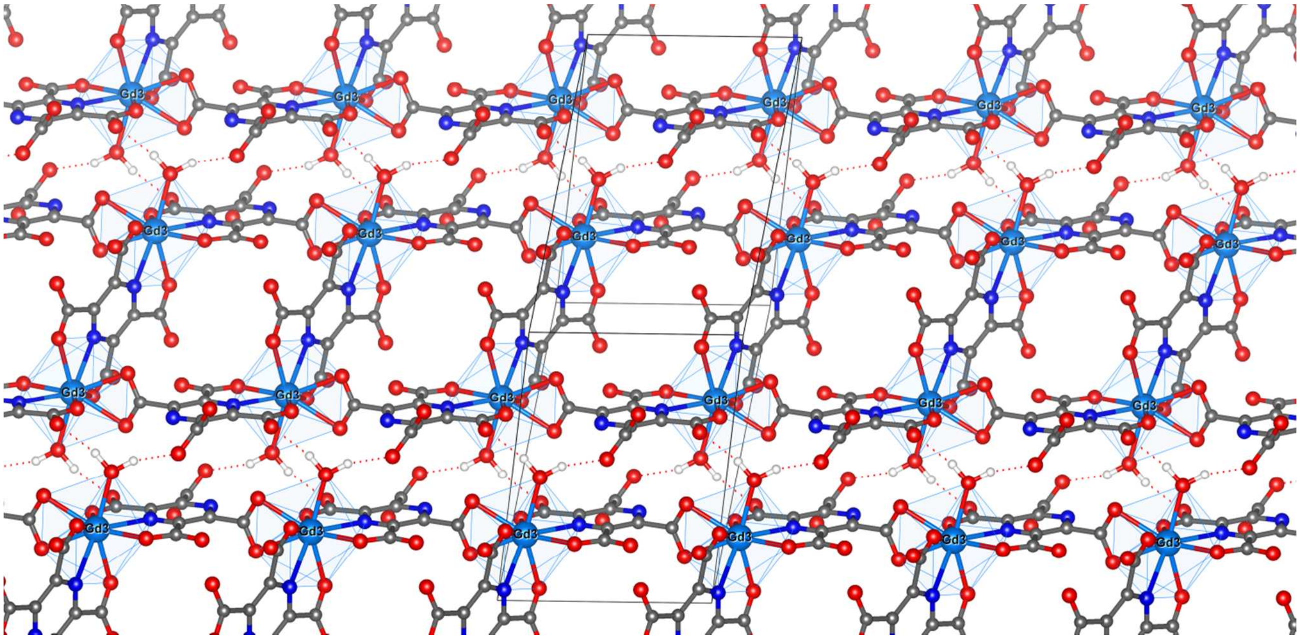

Fig. 6b

Fig. 6. A subnet consisting of infinite one-dimensional chains of gadolinium ions (Gd2) along the crystallographic direction [100] (a). These chains are hydrogen bonded to each other *via* coordinated water molecules to form an infinite two-dimensional layer in the *ab*-plane (b).

Further complex connectivity between pztc and Gd ions are present in the other directions, generating multi-atom bond circuits which are comprised of oxygen and carbon atoms and the four inequivalent Gd ions. A 3-D open framework structure with irregular shaped channels along the crystallographic direction [001] results, which is approximately 12 Å as the widest part dimension (Fig. 7). Void analysis using PLATON[47] indicates that, the total solvent accessible volume is 20 % of the total volume and 25 % of the total volume with coordinated water removed, which is consistent with the amount of solvent molecules from elemental and thermogravimetric analyses.

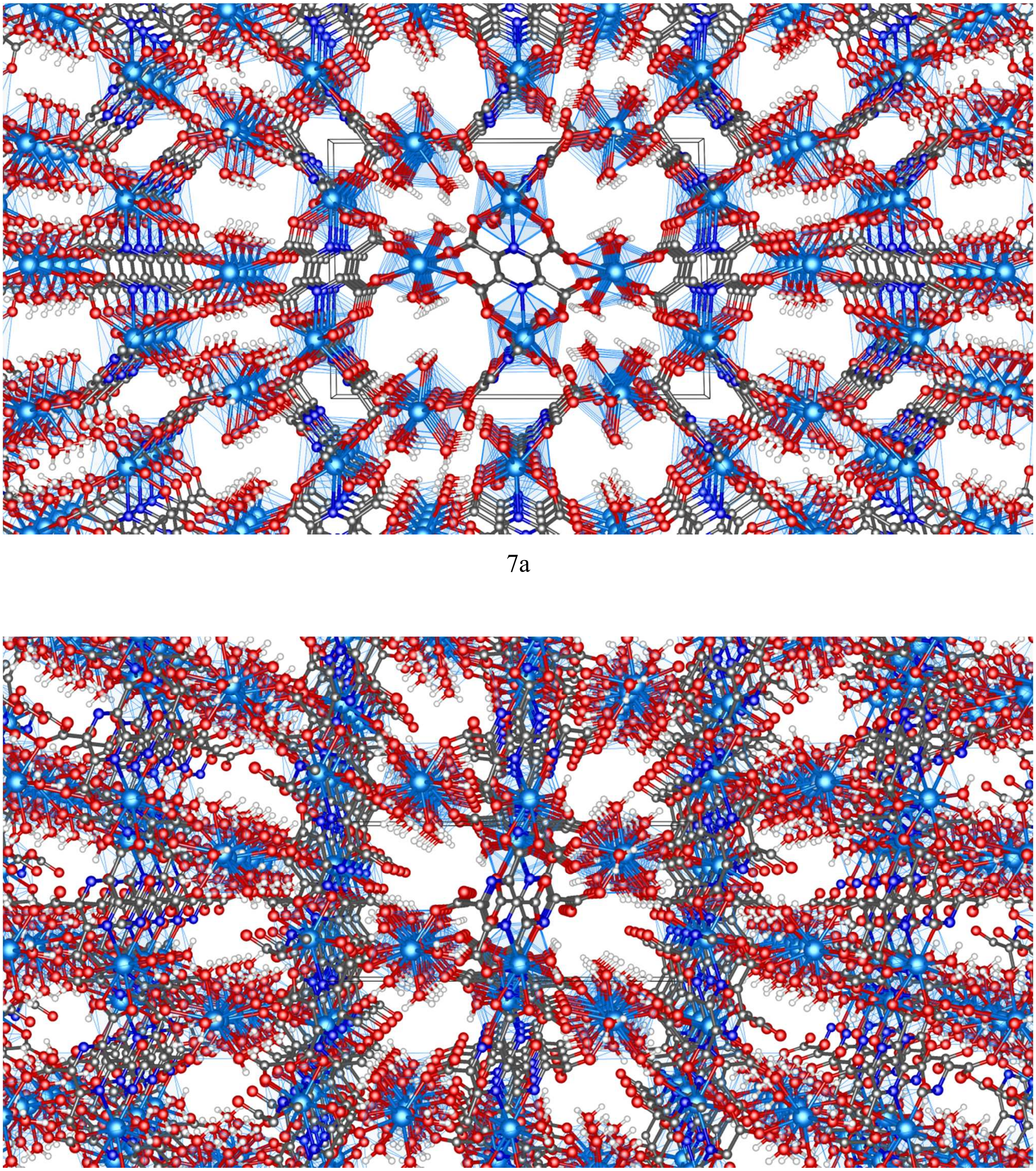

7a

7b

Fig. 7. A diagram of the 3-D framework with perspective projected onto a) the (001) plane and b) the (010) plane.

The decadentate coordination (Fig. 3a) is extremely rare for this ligand in MOFs and CP structures.[24,31] In heptadentate coordination, two oxygen atoms from two different CO_2 groups, and a nitrogen atom at position 4 do not coordinate to Gd (Fig. 3b). Non-coordinated oxygen atoms form strong hydrogen bonds (of comparable strength to Gd) with water molecules. It appears that the pztc^4 and Gd(III) ions are well suited for both forming hydrogen bonds to water and for forming bonds to each other. The small partial charge on the oxygen atoms in this ligand allows bonds of comparable strength to be formed to Gd and water molecules. Thus cluster units $[Gd(ptz\underline{c})_2(H_2O)_6]$, $[Gd(ptz\underline{c})_2(H_2O)_4]$, $[Gd(ptz\underline{c})_3(H_2O)_3]$, $[Gd(ptz\underline{c})_3(H_2O)]$, and $[Gd(ptz\underline{c})_4]$, coexist in the structure. Higher coordination numbers for the ligand appears to be more stable than lower coordination numbers. Possibly, heptadentate, instead of decadentate, coordination occurs to provide hydrogen bond acceptors for the coordinated water molecules in the absence of other water molecules. Steric hindrance from the ligand's carboxylates, that is reported to inhibit tridentate -ONO- coordination in related compounds as expressed by other researchers,[22] is not a significant factor in this case.

The structures crystallize in a triclinic system, *P*-1 space group, which is also observed for 3-D Cd pztc MOF[24]. The space group is however, different from other pztc-coordination polymers in which triclinic system, *P*1[8,9] and monoclinic system, $P2_1/c$ space groups[33] are present, for example. The 3-D MOFs lanthanide-pztc that are reported by Quan *et al.* [33] share the unusual bis-tridentate -ONO- chelation of the pztc**,** but possess significant differences in metal-pztc-H_2O ratios, 3-D connectivity and space group, than those that are present in **1** and **2**.

The varied and multidirectional connectivity of the pztc in these lanthanide structures is striking and the loss of symmetry is significant. However, it is not clear how the interplay between the chemical and symmetry restrictions produces this complex network structure. It is clear that the variations occur because the metal centers are large and because the interactions between the metal ions and the ligands are primarily electrostatic. The absence of electronic effects at the Gd atom and its large size places fewer restrictions on the bond angles. This leads to the open, 3-D network. Interestingly, the crystal structure might be regarded as a composite structure consisting of three different coordination polymers (Gd1, Gd2, and Gd3) and discrete $[Gd4(pztc)_2(H_2O)_6]$ units. These four structural elements coexist in a single crystal structure. Each of these motifs resembles the structures of standard transition metal polymers.

Simplifying the structure using TOPOS[48] reveals a network structure with Gd atoms and the ligands as nodes. To derive the simplified net, centers of the μ_4-heptadentate and decadentate pyrazine groups are reduced to 4-coordinate nodes, the μ_3-heptadentate ligands are 3-coordinate nodes, and the Gd2 and Gd4 atoms 2-coordinate nodes in the structure. The 2-connected nodes are linear linkers which do not affect the overall topology. Only 3-connected and higher order nodes are considered when evaluating the topology of an MOF structure. This network is simplified further by removing the intervening 2-coordinate Gd linkers to generate a 3,3,4,4,4,4-coordinate, 6-nodal net. (Figs. 8a and 8b).

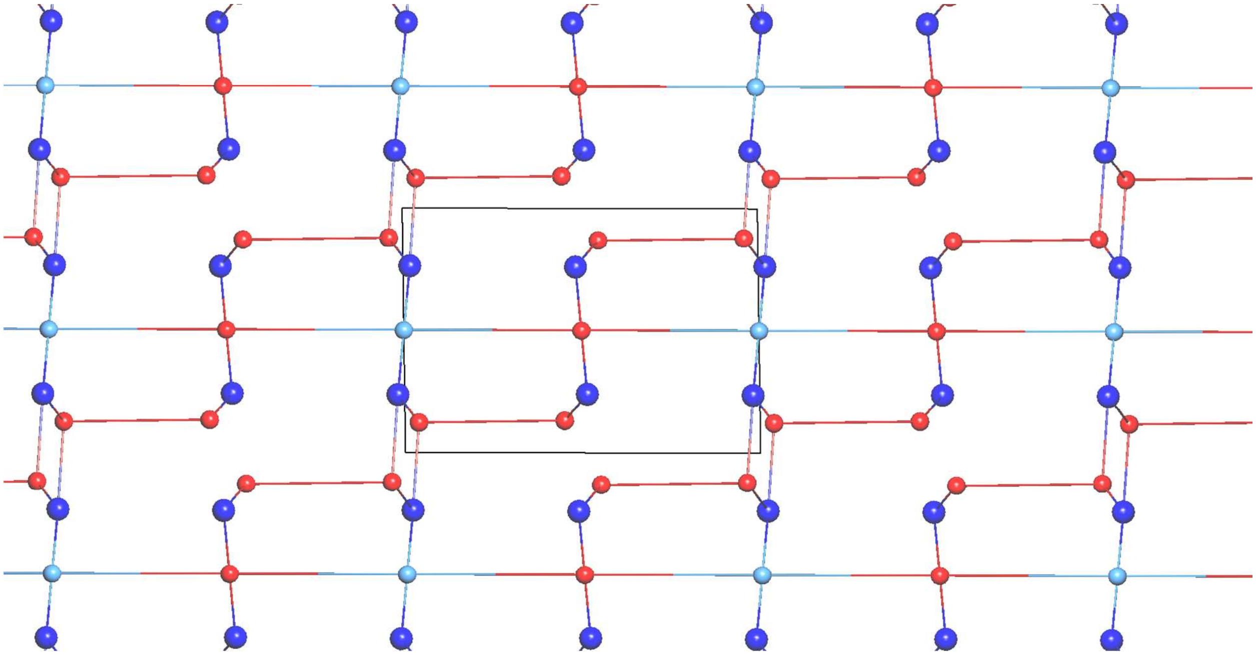

8a

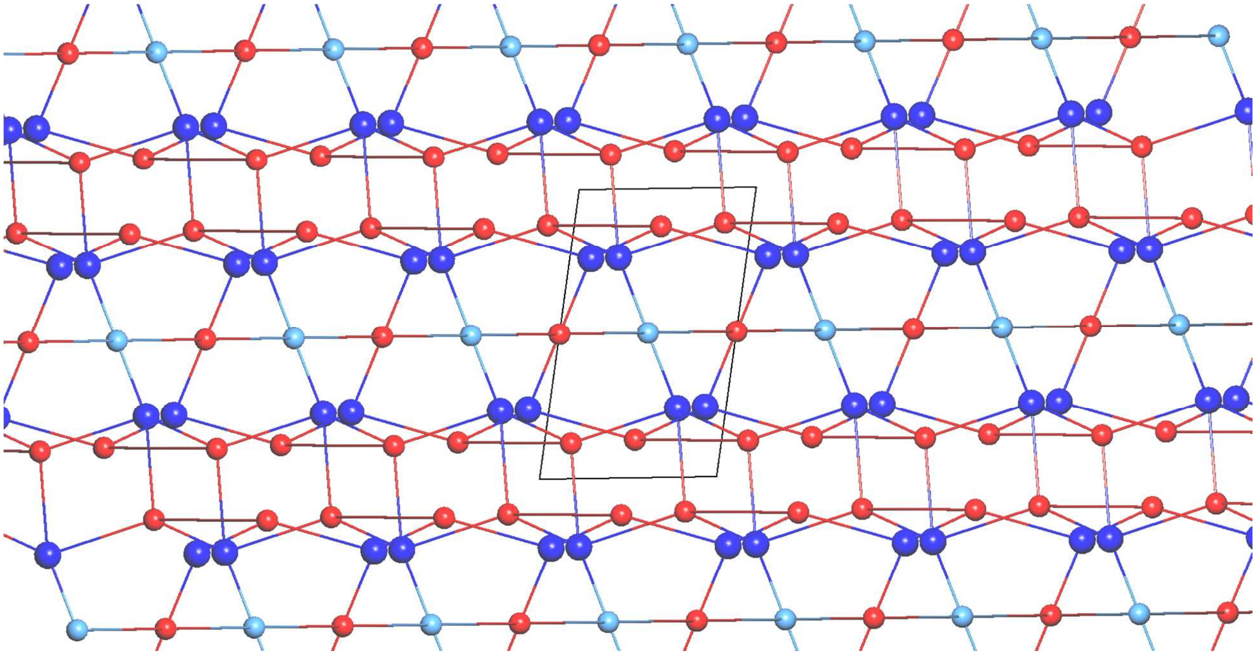

8b

Fig. 8. The underlying topology of the coordination network, showing 6-nodal net in compound **1**. The nodes corresponding to the μ_3 and μ_4 ligands are show as spheres.

The channels and voids contain tightly hydrogen-bonded non-coordinated water. Non-coordinated water molecules are hydrogen bonded to each other, to the coordinated water molecules, and also to oxygen atoms of selected ligand carboxylates that are within close proximity. The hydrogen bonding network of water molecules is extensive and further stabilizes the structure. Using the bond valence model, the nine-coordinate Gd(III) forms bonds of -0.33 v.u. each to nine oxygen atoms. Each of the two hydrogen atoms of the coordinated water molecule donates an external hydrogen bond of 0.17 units to another water molecule or to a non-coordinated oxygen atom from pztc. This hydrogen bond strength is similar to that of liquid water and a single coordination sphere with hydrogen bonded water molecules about Gd(III) is stable. The hydrogen bond O···H bond distances ranged from 1.68 Å (H6WB-O18W) to 2.14 Å (H20A-010W) while the O---O distances (which are more precisely determined) are in the range 2.638(5) to 2.893(5) Å. These O—O distances (Table 3) are within the range reported for hydrogen bonds in a related lanthanide structure [33] and similar to those in liquid water and ice (2.82 Å).

PXRD patterns: The PXRD patterns of **1** and **2** were recorded to investigate the phase purity of each structure. The diffraction patterns are almost identical to each other and also match that of the simulated pattern from single crystal x-ray crystallography (Fig. S2), thus further confirming the isostructural nature of both. This also confirms that each structure crystallizes as a pure phase.

FTIR spectra

The FTIR spectra of H_4pztc, **1** and **2** were acquired and compared (Fig. S3). The peak around 1700 cm^{-1} in the spectrum of H_4pztc ligand disappears in the spectrum of **1** due to the formation of (CO_2)Gd bonds, and shows that the ligand is fully deprotonated within the structure. The broad absorption bands at 3420 cm^{-1} and 3200 cm^{-1} are attributed to the O-H vibrations of coordinated water and the water of crystallization. The ν_{as}(C=O) absorption for the ligand at 1730 cm^{-1} and 1659 cm^{-1} redshift to 1629 cm^{-1} in **1** due to the formation of partial bond between oxygen atom and the Gd(III) ion which reduces the bond strength of C=O. In addition, **1** exhibits ν_s(C=O) absorption at 1406 cm^{-1} and 1328 cm^{-1}. The C-O stretching vibrations are observed at 1140 cm^{-1} and 1174 cm^{-1} in the pure ligand and at 1160 cm^{-1} in **1**.

Thermal properties

The thermal properties of **1** and **2** were assessed from their respective TGA curve (Fig. S4). For **1**, the first weight loss event starts at room temperature and ends at 190°C, accounting for 21% of the total sample weight and corresponding to the loss of twenty one molecules of coordinated and lattice H_2O (calc. 22 %). A second major weight loss event of 35 % occurs between 450°C and 700°C and is attributed to the decomposition of the ligand. The final residue of 45 wt % is attributed to Gd_2O_3 (calc. 41 %). The TGA data correlates well with elemental and x-ray single crystal analysis. The thermogravimetric curve of **2** shows similar weight loss features.

Magnetic properties

Temperature – dependent magnetic susceptibilities were measured between 5K to 320 K for **1** and **2.** The χ and χT values versus temperature are both plotted, where χ is the molar magnetic susceptibility per molecular unit (Fig. 9). The temperature-dependent susceptibility curves for both **1** and **2** obey the Curie-Weiss law and show that the lanthanide ions exhibit paramagnetic behavior in the structures. For **1**, the χT value remains constant at a value of 35 cm^{3}Kmol^{-1} (with S = 3.5, L = 0, J = 3.5 and g_J = 2) over the temperature range investigated (Fig. 9a inset). This is consistent with the theoretical value[49] of 31.5 cm^{3}Kmol^{-1} for four isolated non-interacting Gd(III) ions, and suggests that the interatomic distances are outside of the range within which Gd…Gd magnetic interactions can occur.

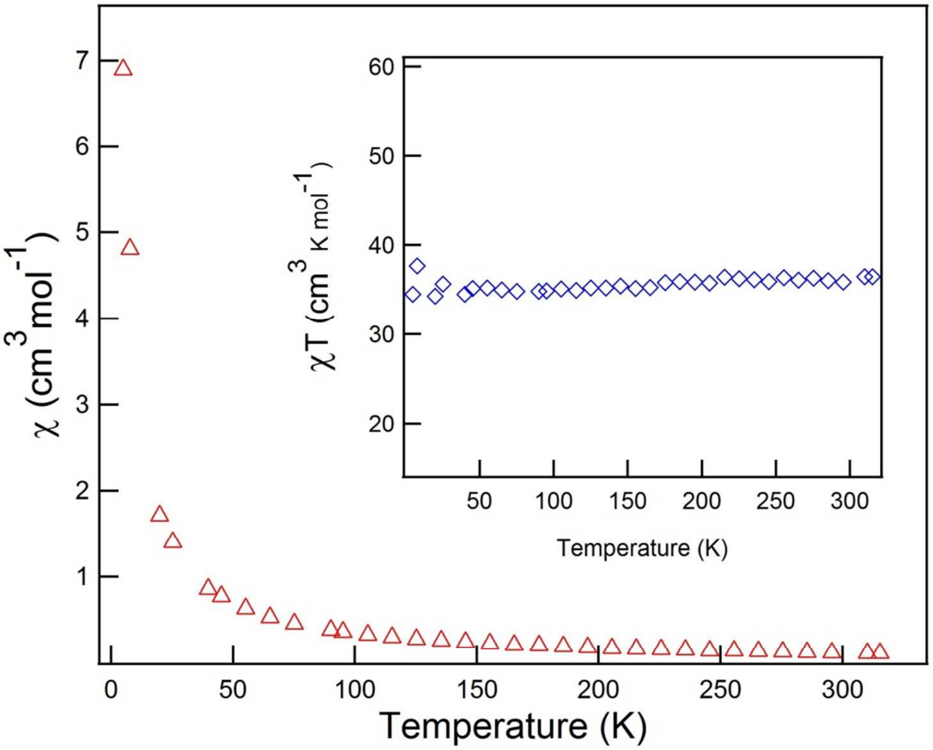
χ (cm^3 mol^{-1})
Temperature (K)
χT (cm^3 K mol^{-1})
Temperature (K)

Fig. 9a

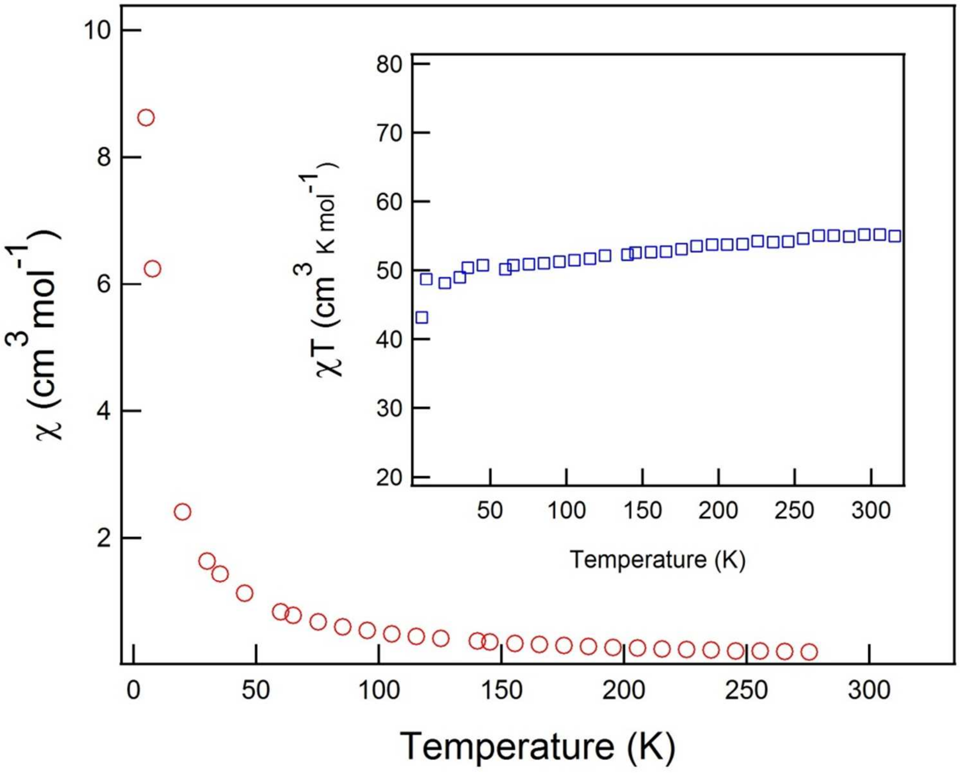
χ (cm^3 mol^{-1})
Temperature (K)
χT (cm^3 K mol^{-1})
Temperature (K)

Fig. 9b.

Fig. 9. Magnetic susceptibility vs temperature plots for **1** (a) and **2** (b).

For **2**, the average χT can be considered as around 52 cm^{3}mol^{-1}K (Fig. 9b) (with S = 3, L = 3, J = 6 and g_J = 1.5) and compares well with the theoretical spin only value of 47.2 cm^{3}mol^{-1}K for four non interacting Tb(III) ions.[49] Also, an abrupt decrease of χT below 10 K is observed, suggesting some possible electron transition and/or magnetic interactions on metal centers with changing temperature. Surely, it is fundamentally very interesting and detailed studies should be further conducted.

Conclusion

Two new isostructural open 3-D lanthanide organic frameworks, $[Ln_4(C_8N_2O_8)_3(H_2O)_{11}]\bullet 10(H_2O)$ (Ln= Gd and Tb) were synthesized under hydrothermal conditions using the ligand, pyrazine-2,3,5,6-carboxylic acid. The fully deprotonated ligand coordinates four crystallographically distinct lanthanide ions in decadentate or heptadentate modes. There is a delicate interplay of hydrogen bonding (between water molecules only and between pztc and water molecules) and, ligand to Ln(III) coordinate bonding. This yields a complex three-dimensional structure with four distinct Ln(III) ions and four different pztc ligands with varied ligand coordination modes. This combination of coordination modes is new for this ligand in MOFs and CP structures. The combination of the deprotonated ligand of high denticity, and the lanthanide metal ions with their propensity for high coordination, promotes intricate 3-D connectivity, leading to open framework structure with channels. The channels contain hydrogen bonded non-coordinated guest water molecules. The magnetic behavior of the structures is characteristic of the respective isolated paramagnetic lanthanide ions. The results demonstrate the versatility of the multidentate pztc ligand in the design and synthesis of lanthanide MOFs.

Electronic Supplementary Information (ESI) available: TGA curves, FTIR spectra, PXRD patterns, and the lists of bond lengths, bond angles and other structural details are provided as ESI. Crystallographic data for the structural analysis have been deposited with the Cambridge Crystallographic Data Center as CCDC Nos. 1035324 and 1035325 for **1** and **2** respectively. These data can be obtained online free of charge via http://www.ccdc.cam.ac.uk/pages/Home.aspx (or from Cambridge Crystallographic Data Centre, 12 Union Road, Cambridge CB21EZ, UK, or www.deposit@ccdc.cam.ac.uk).

Acknowledgements: J. B. acknowledges discussions with I. David Brown on the bonding of pyrazine-2,3,5,6-tetracarboxylate and water molecules with Gd(III). He also acknowledges discussions with V.A. Blatov at Samara State University on the topological analysis using TOPOS. This work was supported by United States National Science Foundation Grants Nos. HRD-0630456 and HRD-1305041, and United States National Nuclear Security Administration Grant No. NA0000979.

Table 1. Crystallographic data and processing parameters for **1** and **2**

Identification	**1**	**2**
Empirical formula	$C_{24}H_{42}Gd_4N_6O_{45}$	$C_{24}H_{42}Tb_4N_6O_{45}$
Formula weight	1763.63	1770.31
Temperature/K	110(2)	110(2)
Crystal system	triclinic	triclinic
Space group	*P*-1	*P*-1
a/Å	8.5607(10)	8.5627(15)
b/Å	14.1023(17)	14.078(3)
c/Å	20.294(2)	20.297(3)
α/°	88.5392(17)	88.568(3
β/°	86.4998(15)	86.325(4)
γ/°	81.2519(16)	81.382(3)
Volume/$Å^3$	2416.6(5)	2413.82
Z	2	2
ρ_{calc}mg/mm^3	2.426	2.436
μ/mm^{-1}	5.553	5.923
F(000)	1686	1696
Crystal size/mm^3	0.39×0.15×0.11	0.83 x 0.11 x 0.03
Θ range for data collection	2.011° to 33.346°	1.463° to 26.732°
Index ranges	-13<=h<=13, -21<=k<=21, -31<=l<=31	-10<=h<=10, -17<=k<=17, -25<=l<=25
Reflections collected	24173	19021
Independent reflections	17134 [R(int) = 0.0571]	10146[R(int) = 0.1810]
Data/restraints/parameters	14301/238 /809	10146/874/781
Goodness-of-fit on F^2	1.055	0.971
Final R indexes [I>=2σ (I)]	R_1 = 0.0571, wR_2 = 0.1454	R_1=0.1360, wR_2 =0.2557
Final R indexes [all data]	R_1 = 0.0691, wR_2 = 0.1514	R_1=0.2457, wR_2 =0.2983
Largest diff. peak/hole / e $Å^{-3}$	4.727 / -5.902	4.694/-4.535

Table 2. Selected interatomic distances (Å) and bond angles (°) with their estimated standard deviations (x 103 Å, x 10°)) in $\{[(Gd_4(C_8N_2O_8)_3(H_2O)_{11}]\bullet 10(H_2O)\}_n$

Bond lengths	
Gd(1)-O(1)	2.385(3)
Gd(1)-O(5)	2.394(3)
Gd(1)-O(7)	2.482(3)
Gd(1)-N(1)	2.610(3)
Gd(1)-N(5)	2.519(3)
Gd(1)-O(9)#1	2.438(3)
Gd(1)-O(10)#1	2.506(3)
Gd(1)-O(11)#2	2.344(3)
Gd(1)-O(4)#3	2.366(3)
Gd(2)-O(1W)	2.364(3)
Gd(2)-O(2)	2.413(3)
Gd(2)-O(2W)	2.347(3)
Gd(2)-O(3)	2.333(3)
Gd(2)-O(3W)	2.360(3)
Gd(2)-O(4W)	2.376(4)
Gd(2)-O(13)	2.421(3)
Gd(2)-O(16)#4	2.351(3)
Gd(3)-O(9W)	2.400(3)
Gd(3)-O(14)	2.427(3)
Gd(3)-O(15)	2.403(3)
Gd(3)-O(19)	2.407(3)
Gd(3)-O(21)	2.376(3)
Gd(3)-N(2)	2.662(3)
Gd(3)-N(3)	2.520(3)
Gd(3)-O(23)#5	2.490(3)
Gd(3)-O(24)#5	2.464(3)
Gd(4)-O(5W)	2.507(3)
Gd(4)-O(6W)	2.457(3)
Gd(4)-O(7W)	2.447(3)
Gd(4)-O(8)	2.442(3)
Gd(4)-O(8W)	2.512(3)
Gd(4)-O(17)	2.338(3)
Gd(4)-O(20)	2.541(3)
Gd(4)-O(20W)	2.394(3)
Gd(4)-O(21W)	2.438(3)
Bond angles	
O(9)-Gd(1)-O(10)	53.20(10)
O(1)-Gd(1)-N(1)	62.31(10)
O(13)-Gd(1)-O(14)	82.50(10)
O(10)-Gd(1)-O(14)	75.93(11)
O(1)-Gd(1)-N(1)	62.31(10)
O(1W)-Gd(2)-O(3W)	84.89(11)
O(1W)-Gd(2)-O(2)	77.29(11)
O(13)-Gd(2)-O(16)	70.64(11)
O(23)-Gd(3)-O(24)	53.31(11)
O(24)-Gd(3)-N(2)	66.98(10)
O(15)-Gd(3)-O(21)	77.25(11)
O(6W)-Gd(4)-O(7W)	70.47(10)
O(6W)-Gd(4)-O(8)	66.80(10)
O(17)-Gd(4)-O(20)	69.97(10)

[1]3-X,1-Y,-Z; [2]-1+X,+Y,+Z; [3]2-X,1-Y,1-Z; [4]1+X,+Y,+Z; [5]2-X,2-Y,-Z

Table 3. Selected hydrogen bond distances (Å) and angles (°) with their estimated standard deviations (x 10^3 Å, x 10°) in $\{[(Gd_4(C_8N_2O_8)_3(H_2O)_{11}]\bullet 10(H_2O)\}_n$

D-H...A	d(D-H)	d(H...A)	d(D...A)	<(DHA)
O(1W)-H(1WA)...O(12W)	1.007(7)	1.804(7)	2.809(4)	176.6(14)
O(1W)-H(1WB)...O(16W)	0.985(7)	1.713(7)	2.684(5)	168.0(10)
O(2W)-H(2WA)...O(18W)	0.984(8)	1.781(11)	2.736(5)	162.7(13)
O(3W)-H(3WB)...O(15W)	0.985(8)	1.733(9)	2.709(5)	170.1(12)
O(4W)-H(4WA)...O(19W)	0.981(7)	1.691(9)	2.638(5)	160.7(14)
O(4W)-H(4WB)...O(22)#8	0.986(7)	1.713(8)	2.685(4)	168(3)
O(5W)-H(5WA)...O(10)#5	1.008(7)	1.957(10)	2.809(4)	140.5(8)
O(6W)-H(6WA)...O(11)	0.996(7)	1.842(8)	2.834(5)	174.3(13)
O(6W)-H(6WB)...O(18W)	0.984(7)	1.684(8)	2.638(5)	162.1(11)
O(21W)-H(21A)...O(12)	0.975(4)	1.933(5)	2.890(4)	166.3(8)
O(10W)-H(10A)...O(14)	0.986(7)	1.855(8)	2.807(4)	161.3(10)

^{1}1-X,2-Y,1-Z; ^{2}1+X,-1+Y,+Z; ^{3}2-X,1-Y,-Z; ^{4}1+X,+Y,+Z; ^{5}2-X,1-Y,1-Z; ^{6}1-X,2-Y,-Z; ^{7}-1+X,+Y,+Z; ^{8}-1+X,1+Y,+Z; ^{9}-X,2-Y,1-Z

References

---

1 (a) J.- R. Li, J. Sculley, and H.- C. Zhou, *Chem. Rev.*, 2012, **112** (2), 869–932. (b) R. Heck, J. Bacsa, J. E. Warren, M. J. Rosseinsky and D. Bradshaw, *CrystEngComm*, 2008, **10**, 1687-1692. (c) J. B. DeCoste and G. W. Peterson, *Chem. Rev.*, 2014, **114** (11), 5695–5727. (d) M. Eddaoudi, J. Kim, N. Rosi, D. Vodak, J. Wachter, M. O'Keeffe and O.M. Yaghi, *Science*, 2002, **295**, 469-472. (e) Y.- C. He, H.- M. Zhang, Y.- Y. Liu, Q.- Y. Zhai, Q.- T. Shen, S.- Y. Song, and J.- F. Ma, *Cryst. Growth Des.*, 2014, **14** (7), 3174–3178. (f) J. Yu, Y. Cui, C.- D. Wu, Y. Yang, B. Chen, and G. Qian, *J. Am. Chem. Soc.*, 2015, **137** (12), 4026 - 4029.

2 (a) J. Liu, L. Chen, H. Cui, J. Zhang, L. Zhang and C.- Y. Su, *Chem. Soc. Rev.*, 2014, **43**, 6011-6061. (b) A. Corma, H. Gracia and F. X. Llabres I Xamena, *Chem. Rev.*, 2010, **110**, 4606-4655. (c) L. Alaerts, E. Seguin, H. Poelman, F. Thibault-Starzyk, P. A. Jacobs and D. E. De Vos, *Chem-Eur. J.*, 2006, **12** (28) 7353-7363. (d) F. Vermoortele, R. Ameloot, A. Vinmont, C. Serre and D. E. DeVos, *Chem. Commun.*, 2011, **47**, 1521-1523. (e) B. Dutcher, M. Fan and A. G. Russell, *ACS Appl. Mater. Interfaces*, 2015, **7** (4), 2137- 2148.

3 (a) K. C. Stylianou, J. E. Warren, S. Y. Chong, J. Rabone, J. Bacsa, D. Bradshaw and M. J. Rosseinsky, *Chem. Commun.*, 2011, **47**, 3389-3391. (b) M. P. Suh, H. J. Park, T. K. Prasad and D.- W. Lim, *Chem. Rev.*, 2012, **112,** 782-835. (c) J.- R. Li, J. Sculley, and H.-C. Zhou, *Chem. Rev.*, 2012, **112,** 869-932. (d) J. L. C. Roswell and O. M. Yaghi, *Angew. Chem. Int. Ed.*, 2005, **44**, 4670-4679. (e) M. Latroche, S. Surble, C. Serre, C. Mellot-Draznieks, P. L. Llewellyn, J. H. Lee, J. S. Chang, S. H. Jhung and G. Ferey, *Angew. Chem. Int. Ed.*, 2006, **45**, 8227-8231.

4 (a) S. I. Swamy, J. Bacsa, J. T. A. Jones, K. C. Stylianou, A. Steiner, L. K. Ritchie, T. Hasell, J. A. Gould, A. Laybourn, Y. Z. Khimyak, D. J. Adams, M. J. Rosseinsky and A. I. Cooper, *J. Am. Chem. Soc.*, 2010, **132** (37), 12773-12775. (b) L. E. Kreno, K. Leong, O. K. Farha, M. Allendorf, R. P. Van Duyne and J. T. Hupp, *Chem. Rev.*, 2012, **112**, 1105-1125. (c) K. Koh, A. G. Wong-Foy and A. J. Matzger, *J. Am. Chem. Soc.*, 2009, **131**, 4184-4185. (d) D. Zhao, D. Yuan, D. Sun and H.- C. Zhou, *J. Am. Chem. Soc.,* 2009, **131**, 9186-9188. (e) J. Rocha, L. D. Carlos, F. A. Almeida Pas and D. Ananias, *Chem. Soc. Rev.*, 2011, **40**, 926-940. (f) Y. Cui, B. Chen, G. Qian, *Coord. Chem. Rev.*, 2014, **273–274**, 76–86. (g) M. D. Allendorf, C.A. Bauer, R. K. Bhakta and R. J. T. Houk, *Chem. Soc. Rev.*, 2009, **38**,1330-1352.

5. (a) W. Starosta and J. Leciejewicz, *Acta Crystallogr. Sect. E*: *Struct. Rep. Online*, 2010, **12**, 1561-1562. (b) W. Starosta and J. Leciejewicz, *Acta Crystallogr. Sect. E*: *Struct. Rep. Online,* 2014, **70** (6), 234-235.

---

6 W. Starosta and J. Leciejewicz, *Acta Crystallogr. Sect. E: Struct. Rep. Online,* 2014, **70** (5), 172-173.

7 B. Masci, S. Pasquale and P. Thuéry, *Cryst. Growth Des.*, 2010, **10**, 2004-2010.

8 W. Starosta and J. Leciejewicz, *J. Coord. Chem.*, 2008, **61**, 490-498.

9 M. Gryz, W. Starosta and J. Leciejewicz, *Acta Crystallogr. Sect. E: Struct. Rep. Online*, 2005, **61**, 1920-1922.

10 S. K. Ghosh and P. K. Bharadwaj, *Eur. J. Inorg. Chem.*, 2005, **24**, 4880-4885.

11 S. K. Ghosh and P. K. Bharadwaj, *Inorg. Chem.*, 2004, **43**, 6887-6889.

12 S. K. Ghosh, M. S. El Fallah, J. Ribas and P. K. Bharadwaj, *Inorg. Chim. Acta.*, 2006, **359**, 468-474.

13 A. H. Yang**,** Y. P. Quan, L.H. Zhao, J. Z. Cui, H. L. Gao, F. L. Lu, W. Shi and P. Cheng, *J. Coord. Chem.*, 2009, **62** (20), 3306-3313.

14 A. H. Yang, Y. P. Quan, H. L. Gao, S. R. Fang, Y. P. Xhang, Li. H. Zhao, J. Z. Cui, J. H. Wang, S. Wei, and P. Cheng, *CrystEngComm*, 2009, **11 (**12), 2719-2727.

15 M. V. Yigit, Y. Wang, B. Moulton and J. C. MacDonald, *Crystal Growth Des.*, 2006, **6** (4), 829-832.

16 M. Graf, H. Stoeckli-Evans, C. Whitaker, P. A. Marioni and W. Marty, *Chimia*, 1993, **47** (6), 202-205.

17 H. L. Gao, Y. P. Zhang, A. H. Yang, S. R. Fang and J. Z. Cui, *J. Mol. Struct.*, 2009, **918**, 97-100.

18 P. A. Marioni, W. Marty, H. Stoeckli-Evans and C. Whitaker, *Inorg. Chim. Acta.*, 1994, **219**, 161-168.

19 F. F. Li, Q. Q. Zhang, Y. Y. Zhao, S. X. Jiang, X. Y. Shi, J. Z. Cui and H. L. Gao, *RSC Adv.*, 2014, **4**, 10424-10433.

20 P. A. Marioni, H. Stoeckli-Evans, W. Marty, H. U. Guedel and A. F. Williams, *Helv. Chim. Acta.*, 1986, **69**, 1004-1011.

21 L. H. Zhao, Y. P. Quan, A. H. Yang, J. Z. Cui, H. L. Gao, F. L. Lu, W. Shib and P. Cheng, *CrystEngComm.* 2009, **11**, 1427-1432.

22 M. Alfonso, A. Neels and H. Stoeckli-Evans, *Acta Crystallogr. Sect. C: Cryst. Struct. Commun.*, 2001, **C57**, 1144-1146.

23 T. Guethner and U. Thewalt, *J. Organomet. Chem.,* 1989, **371**, 43-56.

24 L.-H. Zhao, A. H. Yang, Y. P. Quan, H. L. Gao and J. Z. Cui, *J. Chem. Crystallogr.*, 2011**, 41**, 1245-1248.

25 S. K. Ghosh and P. K. Bharadwaj, *J. Mol. Struct.,* 2006, **796**, 119-122.

26 H. S. Wang, W. Shi, J. Xia, H. B. Song, H. G. Wang and P. Cheng, *Inorg. Chem. Commun.*, 2007, **10**, 856-859.

27 J. Qu, Y. L. Yi, Y. M. Hu, W. T. Chen, H. L. Gao, J. Z. Cui and B. Zhai, *J. Coord. Chem.*, 2012, **65**, 3740-3751.

28 F. Zhang, P. Yan, X. Zou, J. Zhang, G. Hou and G. Li, *Cryst. Growth Des.*, 2014, **14**, 2014-2021.

29. F. Zhang, P. Yan, H. Li, X. Zou, G. Hou and G. Li, *Dalton Trans.*, 2014, **43**, (33), 12574-12581.

30 P. Thuery and B. Masci, *CrystEngComm,* 2010, **12**, 2982-2988.

31 B. Masci and P. Thuery, *Cryst. Growth Des.*, 2008, **8**, 1689-1696.

32 A. H. Yang, H. L. Gao and J. Z. Cui, *Inorg. Chem. Commun.*, 2010, **13**, 1309-1313.

33 Y. P. Quan, L-H. Zhao, A. H. Yang, J. Z. Cui, H. L. Gao, F-L. Lu, W. Shi and P. Cheng, *CrystEngComm*, 2009, **11**, 1679-1685.

34 P. Vishweshwar, N. J. Babu, A. Nangia, S. A. Mason, H. Pushman, R. Mondal and J. A. K. Howard, *J. Phys. Chem*. A, 2004, **108**, 9406-9416.

35 L. Palatinus and G. Chapuis, *J. Appl. Cryst.* 2007, **40**, 786-790.

36 (a) V. Dolomanov, L. J. Bourhis, R. J. Gildea, J. A. K. Howard and H. Puschmann , *J. Appl. Cryst*., 2009, **42**, 339-341. (b) L. J. Barbour, J. *Supramol . Chem*., 2001, **1**, 189-191.

37 G. M. Sheldrick, *Acta Crystallogr. Sect. A: Found. Crystallogr*., 2008, **A64**, 112-122.

38 M. E. Fleet, *Mineral. Mag*., 1976, **40**, 531-533.

---

39 J. E. Huheey, E. A. Keiter, and R. L. Keiter, *Inorganic Chemistry: Principles of Structure and Reactivity*, 4th edn., Harper Collins, New York, 1993.

40 L. Liao, C.W. Ingram, D. Vandeveer, K. Hardcastle, K. M. Solntsev, D. Sabo, Z. J. Zhang and R.T. Weber, *Inorg. Chim. Acta*., 2012, **391**, 1-9.

41 Z. R. Meng, Q. Z. Zhang, X. Y. Wu, L. J. Chen and C. Z. Lu, *Acta Crystallogr. Sect. E: Struct. Rep. Online*, **62**, (7), 1033-1035.

42 H. Li, Z. Niu, T. Han, Z. Zhang, W. Shi, P. Chang, *Sci. China*, 201,**1**, 549, 423-428.

43 R. D. Poulsen, J. Overgaard, M. A. Chevalier, H. F. Clausen, and B. Iverson, *Acta Crystallogr. Sect. E: Struct. Rep. Online*, 2005, **61**, **7**, 1337-1339.

44 H. S. Wanga and W. Q. Zhang, *Acta Crystallogr. Sect. E: Struct. Rep. Online*, 2009, **65** (11), 1271.

45 M. Mato- Iglesias, A. Roca-Sablo, Z. Pálinkás, D. Esteban-Gómez, C. Platas-Iglesias, E. Tóth , A. de Bias and T. Rodriquez-Bias, *Inorg. Chem.,* 2008, **47**, 7480-7851.

46 H. L. Zhua, *Acta Crystallogr. Sect. E: Struct. Rep. Online*, 2012, **68**, 1017.

47 A. L. Speck, PLATON, A Multipurpose Crystallography Tool, Utrecht University, The Netherlands, 2001.

48 V. A. Blatov, A. P. Shevchenko, D.M. Proserpio, *Cryst. Growth Des*., 2014, **14**, 3576-3586.

49 V. Chandrasekhar, P. Bag, W. Kroener, K. Gieb, P. Müller, *Inorg. Chem*., 2013, **52**, 13078−13086.

Graphical Abstract

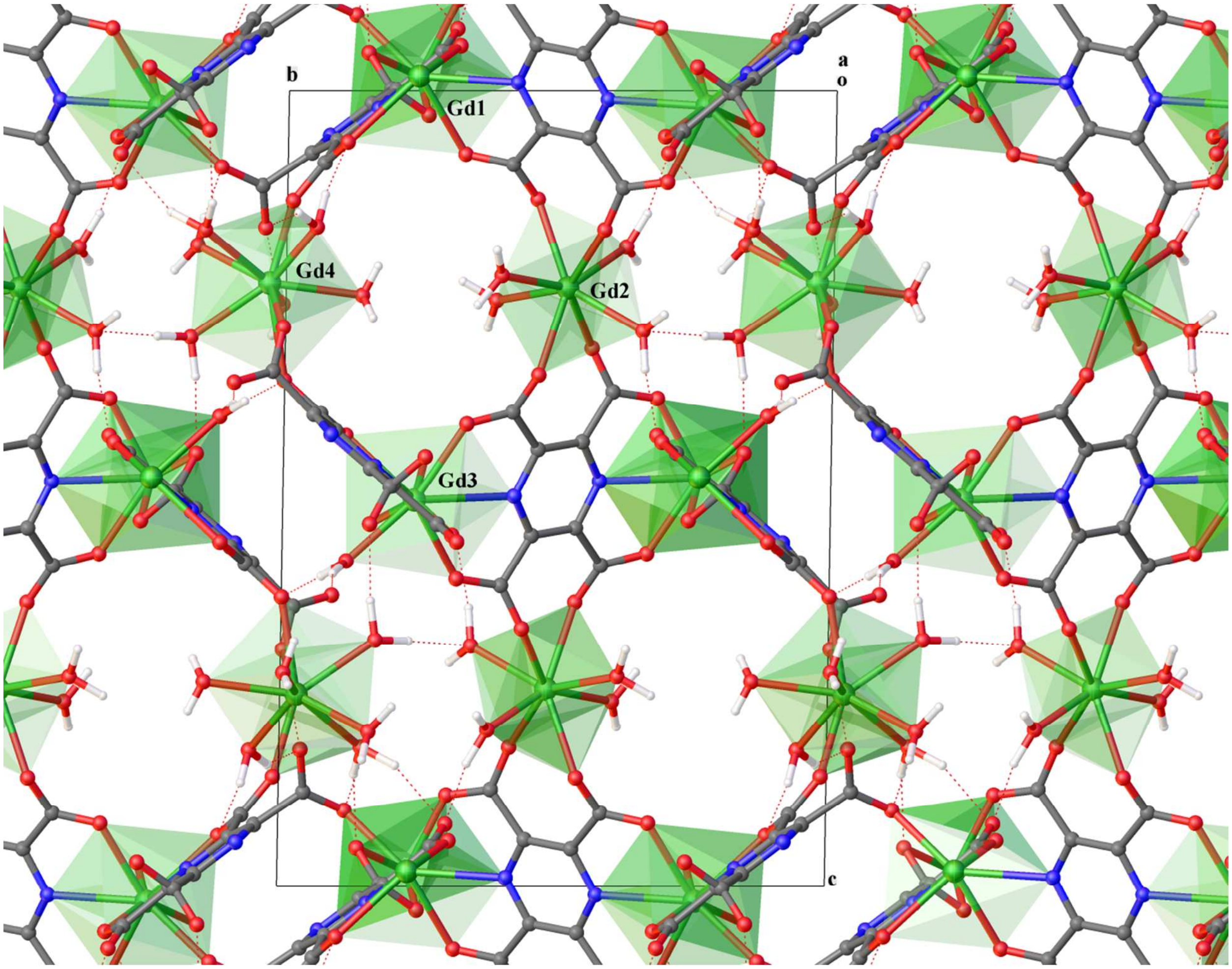

An open 3-D MOF with complex connectivity of multi-topic pyrazine-2,3,5,6-tetracarboxylate linker and Gd(III) atoms. The asymmetric unit contains four symmetry-independent Gd(III) atoms as octa- and nona-coordinate centers, and the fully deprotonated ligand coordinates the Gd (III) through seven or through ten of its atoms. The structure contains irregular channels of approximately 12 Å along the [001] crystallographic direction.